Published in final edited form as:
Arthritis Rheumatol. 2014 January ; 66(1): 152–162. doi:10.1002/art.38225.

An essential role for caspase-1 in the induction of murine lupus and its associated vascular damage

J. Michelle Kahlenberg, M.D., Ph.D.[1,*], **Srilakshmi Yalavarthi, M.S.**[1], **Wenpu Zhao, M.D., Ph.D.**[1], **Jeffrey B. Hodgin, M.D., Ph.D.**[2], **Tamra J. Reed, B.S.**[1], **Noriko M. Tsuji, Ph.D.**[3], and **Mariana J. Kaplan, M.D.**[1,*]

[1]Department of Internal Medicine University of Michigan, Ann Arbor, Michigan, 48109, USA

[2]Department of Pathology, University of Michigan, Ann Arbor, Michigan, 48109, USA

[3]Biomedical Research Institute, National Institute of Advanced Industrial Science and Technology, Tsukuba Central 6-13, Tsukuba, Ibaraki 305-8566, Japan

Abstract

Objective—Systemic Lupus Erythematosus (SLE) is a systemic autoimmune syndrome associated with organ damage and an elevated risk of cardiovascular disease (CVD) resulting from activation of both innate and adaptive immune pathways. Recently, increased activation of the inflammasome machinery in SLE has been described. This study explores if caspase-1, the central enzyme of the inflammasome, plays a role in the development of SLE and its associated vascular dysfunction, using the pristane model of lupus.

Methods—Eight-week old wild-type or caspase-1 −/− mice were exposed to PBS or pristane via intraperitoneal injection. Six months post injection, mice were euthanized and the development of a lupus phenotype and vascular dysfunction was assessed.

Results—While wild-type mice exposed to pristane develop autoantibodies and a strong type I IFN response, mice lacking caspase-1 are significantly protected from these features, including pristane-induced vascular dysfunction. Further, the development of immune-complex glomerulonephritis, prominent after pristane exposure in wild-type mice, is significantly abrogated in caspase-1 −/− mice.

Conclusion—These results indicate that caspase-1 is an essential component in the development of lupus and its associated vascular dysfunction and may play an important role in the cross-talk between environmental exposures and autoimmunity development, thus identifying a novel pathway for therapeutic targeting.

Systemic lupus erythematosus (SLE) is a systemic autoimmune syndrome with severe clinical manifestations and enhanced mortality triggered by immune mediated organ damage and a significant increase in cardiovascular (CV) risk due to premature atherosclerosis(1). An important contributor to development of both systemic lupus and its associated increased

*To whom correspondence should be addressed: Division of Rheumatology, Department of Internal Medicine, University of Michigan, 1150 W. Medical Center Drive, 5520 MRSB1, Ann Arbor, Michigan, 48109. Phone: 734-936-3257; Fax: 734-763-4151; mkahlenb@med.umich.edu and makaplan@umich.edu.

There are no financial conflicts or disclosures.

CV risk is the upregulation of type I interferon (IFN) responses, which influence both innate and adaptive immune processes and promote vascular damage (2–4).

Tetramethylpentadecane, commonly known as pristane, is a naturally occurring hydrocarbon oil that can induce chronic inflammation when introduced into the peritoneal cavity. Pristane injection is recognized as a robust model for lupus development, replicating numerous human manifestations including autoantibody generation, arthritis and severe glomerulonephritis(5). Further, the inflammatory response to pristane results in a strong upregulation of type I IFNs through TLR7 and IRF5 activation, contributing to a lupus-like phenotype(5, 6). Indeed, lack of the type I IFN receptor results in limited TLR7 expression, decreased autoantibody synthesis and hampered recruitment of inflammatory monocytes ($Ly6C^{hi}$) due to decreased synthesis of the chemokine CCL2/MCP-1(7, 8). Thus, this model replicates many phenotypic and functional abnormalities of human SLE and has proven very useful in identifying putative pathogenic mechanisms and environmental triggers in this disease in a type I IFN-dependent system.

The inflammasome is a multimolecular complex comprised of platform molecules, scaffolds and caspase-1, the enzyme responsible for processing of IL-1β and IL-18 to their active forms(9). Activation of the inflammasome results from detection of environmental danger signals, including intracellular bacteria and cholesterol crystals(9). A role for the inflammasome in SLE pathogenesis and organ damage has been recently proposed. The activation of the NLRP3 inflammasome by neutrophil extracellular traps (NETs) and associated LL-37 is enhanced in lupus macrophages(10). Further, immune complexes formed by lupus-associated autoantigens (double-stranded DNA (dsDNA) and ribonucleoprotein (RNP)) and their respective autoantibodies, can activate the inflammasome machinery in monocytes(11, 12). Similar activation of the inflammasome was described following exposure to IFN-α in endothelial progenitor cells (EPCs) in human and murine SLE(4). Because these cells are considered key in promoting vascular repair following an insult to the endothelium, inflammasome activation in this system may promote the enhanced CV risk in patients with SLE(4). However, it remains unclear if the inflammasome or its components serve as crucial mediators of autoimmune responses and organ damage *in vivo* in SLE. Thus, we utilized the pristane-induced lupus model to examine whether the central enzyme of the inflammasome, caspase-1, was required for lupus development and severity.

Materials and Methods

Mice

All animal protocols were reviewed and approved by the University of Michigan's committee on use and care of animals. Breeding pairs of caspase-1 −/− mice were initially obtained from Dr. R.A. Flavell (Yale University) and backcrossed onto the Balb/c background for at least 8 generations. Wild-type (WT) Balb/c and C57Bl/6 mice were obtained from Jackson Labs (Bar Harbor, ME). Breeding pairs of caspase-1 −/− mice on a C57BL/6 background were obtained from Dr. Gabriel Nunez at the University of Michigan. Mice were bred at the University of Michigan. For lupus induction, mice were administered

a single 0.5 ml intraperitoneal injection of PBS (as a control) or pristane (Sigma Aldrich, St Louis, MO) at 8 weeks of age and were euthanized 6 months post injection for listed studies.

EPC quantification and assessment of differentiation

Bone marrow mononuclear cells were quantified by flow cytometry as previously described[1]. Briefly, EPCs were defined as $CD34^+$, $CD309^+$ cells in the lineage negative ($CDD19^-$, $CD3^-$, and $CD45^-$) gate. This number was then extrapolated to calculate the percentage of EPCs in the live cell gate and presented as total number of EPCs/10^6 isolated bone marrow cells. The following Abs were used: CD19-biotin (eBioscience, San Diego, CA), CD3e-Biotin (eBioscience), CD45-PE CY5 (Biolegend); for CD19 and CD3e a streptavidin PE/Cy5-conjugated secondary Ab was used (Biolegend); CD34-FITC(eBioscience); CD309-APC (eBioscience); Annexin V-pacific blue (Biolegend). Flow cytometry analysis was performed using a CyAn ADP Analyzer (Beckman-Coulter, Indianapolis, IN).

Assessment of the capacity of bone marrow-derived EPCs to differentiate into mature ECs was performed as previously described(4). Briefly, bone marrow mononuclear cells were plated onto fibronectin-coated plates (BD, Franklin Lakes, NJ) at a density of 1x10^6 cells/cm2 in EGM-2 Bulletkit media (Lonza, Allendale, NJ), supplemented with 5% heat inactivated FBS. After 7 days in culture, live cells were incubated with FITC-conjugated *Bandeiraea (Griffonia) Simplicifolia* Lectin I (Vector Laboratories Burlingame, CA) and 1'-dioctadecyl-3,3,3',3'-tetramethylindocarbocyanine perchlorate (di)–acetylated LDL (ac-LDL, Biomedical Technologies, Stoughton, MA) for 3 h. To assess EC morphology and expression of mature endothelial markers, cells were analyzed by fluorescent microscopy as described(4). A total of 3 random fields of view were acquired for every triplicate well; images were analyzed using the CellC program (http://www.cs.tut.fi/sgn/csb/cellc/) to quantify mature ECs, which were considered as those that coexpress BS-1 lectin and ac-LDL.

Assessment of endothelium-dependent vasorelaxation

Assessment of endothelium-dependent vasorelaxation was performed as previously reported (13). Briefly, following euthanasia, thoracic aortas were excised and cleaned. The endothelium was left intact, and 2-mm aortic rings were mounted in a myograph system (Danish Myo Technology A/S, Aarhus, Denmark) and bathed with aerated (95% O2/5% CO2) physiological salt solution (PSS). Aortic rings were set at 700 mg passive tension, equilibrated for 1 h with buffer change every 20 min. The vessels were contracted with PSS containing 100mM potassium chloride (KPSS) twice prior to performing contraction/relaxation measurements. Cumulative concentrations of Phenylephrine (PE) (10−9 mol/L to 10−5 mol/L) were added to the bath to establish a contraction concentration-response curve. A phenylephrine concentration corresponding to 80% maximum was added, and contraction was allowed to reach a stable plateau. Endothelium-dependent relaxation was then assessed via graded addition of acetylcholine (Ach) in a cumulative fashion.

Characterization of autoAb and cytokine synthesis

Total serum IgG, anti-dsDNA and anti-RNP Ab levels were quantified by ELISA using commercially available kits (Alpha Diagnostic International, San Antonio, TX), following manufacturer's protocols. Plasma cytokine and chemokine levels were quantified using a custom-designed Milliplex assay on undiluted plasma samples (EMD Millipore, Billerica, MA). IL-18 levels were measured via ELISA (eBioscience).

Proteinuria, renal histopathology and immune complex deposition scoring

Urine samples were collected prior to euthanasia and were assessed for total protein with a Bradford assay (Bio-rad), microalbumin using an Albuwell kit (Exocell, Philadelphia, PA) and creatinine (Cr) using a Creatinine Companion kit (Exocell). Ratios of total protein:Cr and microalbumin:Cr were calculated as an estimate to 24 hour urinary protein excretion. For glomerular immune complex deposition, frozen sections were quantified for C3 and IgG deposition as previously described(13). Briefly, sections were stained with FITC-conjugated anti-C3 (ICL, Portland, OR) and Cy3-conjugated anti-mouse IgG (Sigma) for 1 h at 4°C. DNA was visualized using Hoechst (Invitrogen, Eugene, OR). Immune complexes were scored in a blinded fashion by two independent observers. A scale of 0–3 was assigned for both C3 and IgG deposition based on intensity of signal and scores were multiplied by 2 if the staining diffusely involved the glomeruli. Six glomeruli per mouse were scored and the averaged score for each component (IgG and C3) was added to create the composite score.

To score glomerular inflammation, paraffin embedded cortical sections were sectioned at 3 μm thickness. Periodic Acid Schiff (PAS)-stained sections were examined and graded by one of the authors (JBH) in a blinded manner following procedures previously described by us(13). In brief, a semiquantitative scoring system (0=no involvement, 0.5=minimal involvement of <10%, 1=mild involvement of 10–30% section, 2=moderate involvement (31#x02013;60% of section), 3=severe (>60% of section)) was used to assess 2 different parameters of activity (mesangial hypercellularity and endocapillary cellular infiltrate). An activity index was generated by compiling these scores.

Real Time PCR

Total RNA was purified via Tripure (Roche) from $1x10^6$ peritoneal cells, half of a homogenized spleen or $1x10^6$ bone marrow cells isolated on a Histopaque 1083 (Sigma) gradient. One μg of RNA was transcribed into cDNA using oligodT and MMLV (Invitrogen, Carlsbad, CA) using a MyCycler thermocycler (Bio-Rad, Hercules, CA). Primers for the following transcripts were as follows: *Monocyte chemoattractant protein-1* (*MCP*-1) AGGTCCCTGTCATGCTTCTG (forward), GGATCATCTTGCTGGTGAAT (reverse); *Myxovirus (influenza virus) resistance 1 (Mx1)* GATCCGACTTCACTTCCAGATGG (forward), CATCTCAGTGGTAGTCAACCC(reverse); *IFN regulatory factor 7 (IRF-7)* TGCTGTTTGGAGACTGGCTAT (forward), TCCAAGCTCCCGGCTAAGT (reverse); *IFN-inducible protein 10 (IP-10)* ATCATCCCTGCGAGCCTAT (forward), ATTCTTGCTTCGGCAGTTAC (reverse); *ISG15 ubiquitin-like modifier (ISG15)* CAGAAGCAGACTCCTTAATTC (forward), AGACCTCATATATGTTGCTGTG (reverse); *IFN-γ* AGCGGCTGACTGAACTCAGATTGTA (forward), GTCACAGTTTTCAGCTGTATAGGG (reverse); *β-Actin*

TGGAATCCTGTGGCATCCTGAAAC (forward), TAAAACGCAGCTCAGTAACAGTCCG (reverse); *IL-18* ACTGTACAACCGCAGTAATACGC (forward), AGTGAACATTACAGATTTATCCC (reverse); *IL-1β* CCCTGCAGCTGGAGAGTGTGGA (forward), CTGAGCGACCTGTCTTGGCCG (reverse); caspase-1 GACTGGGACCCTCAAGTTTT (forward), CCAGCAGCAACTTCATTTCT (reverse); *NLRP3* ATGCTGCTTCGACATCTCCT (forward), AACCAATGCGAGATCCTGAC (reverse). ABI PRISM 7900HT (Applied Biosystems) was used for quantitative real-time PCR analysis. Samples were normalized to β-actin and fold change was expressed as pristane-compared to PBS-treated samples.

Characterization of Peritoneal Inflammatory Infiltrate

Peritoneal cells were collected by lavage after euthanasia. Washed cells were incubated with fluorochrome-labeled Abs (CD11b, F4/80, CD11c, CD4, Annexin V, PDCA (Biolegend), Ly6G, Ly6C, CD3e (BD Bioscience), and CD8a (eBioscience)) and analyzed by flow cytometry. Cellular definitions were: Neutrophils as $Ly6G^+/CD11b^+$ in the $F4/80^-$ gate; pDCs as $CD11c^+$, $PDCA^+$ in live cell gate; myeloid DCs as $CD11c^+$, $PDCA^-$ in the live cell gate; inflammatory monocytes as $CD11b^+$, $Ly6C^{hi}$ in $Ly6G^-$ gate, and T cells as $CD3e^+$, $CD4^+$ or $CD3e^+$, $CD8^+$. The final data was expressed as percent of cells positive for the specific marker per 10^6 cells collected.

Characterization of neutrophil NETs

Bone marrow neutrophils were isolated via Percoll gradient based on a previously published protocol(14). 1.5×10^5 cells were adhered onto poly-lysine coated coverslips at 37°C and then treated with 40nM PMA overnight. Cells were washed and stained with murine anti-neutrophil elastase (Abcam, Cambridge, MA) and Hoechst. NETs were visualized via fluorescent microscopy, and counted as previously described by our group(15). Total cell numbers were determined by the number of nuclei present per image, and NETs were determined by counting the number of elongated DNA structures co-staining with elastase and Hoechst.

Statistical Analysis

D'Agostino & Pearson omnibus normality test was used to evaluate Gaussian distribution of the data. Analysis of statistical differences between the means of normally distributed data was evaluated by unpaired Student's T-test and Welch's correction was added when variances were statistically significant as judged by F test to compare variances. Non-normally distributed data was evaluated by a Mann-Whitney test. Logistic regression analysis was used to correlate anti-dsDNA titers with renal inflammation and composite immunofluorescence scoring and [IL-18] with renal inflammation.

Results

Pristane exposure results in upregulation of the inflammasome machinery

Elevated levels of IL-18 and caspase-1 associated with SLE have been described(4, 16, 17), and IL-1β levels are known to be increased in pristane-injected mice(18). In order to confirm

these findings in the pristane lupus model, real-time PCR was used to quantify transcripts from splenocytes isolated from Balb/c mice 6 months after intraperitoneal pristane injection. As shown in Table 1, pristane induces a robust induction of inflammasome-associated transcripts, and a trend for elevated IL-18 and IL-1β in the spleen of wild-type (WT), but not caspase-1 −/−, pristane exposed mice. This suggests that the pristane model replicates the alterations of the inflammasome described in human SLE in a caspase-1 dependent manner and that it is a relevant model to study its effects on lupus pathogenesis.

Inflammatory responses to pristane are intact in wild-type and caspase-1 −/− mice

As pristane-induced lupus depends on recruitment of inflammatory cells, particularly inflammatory monocytes(19, 20), into the peritoneal cavity, we determined if lack of caspase-1 modified inflammatory cell recruitment following pristane exposure. As shown in Figure 1A, the inflammatory response following pristane injection in both wild-type (WT) and caspase-1 −/− Balb/c mice was vigorous. Further analysis showed no difference in plasmacytoid dendritic cell (pDC), myeloid DC, or inflammatory monocyte recruitment to the peritoneal cavity (Figure 1B). An enhanced recruitment of neutrophils was observed in the caspase-1 −/− mice (Figure 1B). Further, no difference between WT and caspase-1 −/− mice was noted in the number or size of peritoneal lipogranulomas following pristane exposure (data not shown). These results indicate that lack of caspase-1 does not significantly alter the recruitment of inflammatory cells into the peritoneal cavity or change the formation of lipogranulomas, which are considered a nidus of chronic inflammatory mediators for disease development(5, 21).

Absence of caspase-1 protects against the development of lupus autoantibodies

In order to determine whether lack of caspase-1 is protective in a lupus model, we examined whether autoantibody production was altered 6 months after pristane exposure in caspase-1 −/− mice compared to WT mice. As shown in Figure 1C, pristane induced a substantial increase in anti-ds-DNA and anti-RNP Abs in WT Balb/c mice 6 months post injection. In contrast, autoantibody production in caspase-1 −/− mice was significantly blunted. Hypergammaglobulinemia, manifested by a rise in total IgG following pristane exposure, was also decreased in the caspase-1−/− mice. Furthermore, levels of circulating inflammatory cytokines, such as IL-6 and IL-17, were lower in PBS- and pristane-treated caspase-1 −/− mice, suggesting an overall reduced inflammatory phenotype (Figure 1D). Unlike studies involving the IRF5 knockout(22), no differences in Th1 vs. Th2 cytokine skewing were observed in WT compared to caspase-1 −/− mice following pristane exposure (Table 2). Overall, these results suggest that lack of capase-1 modifies B cell responses and levels of proinflammatory cytokines and leads to decreased autoantibody formation in response to pristane.

Absence of caspase-1 decreases type I IFN signatures in pristane-induced lupus

Induction of a type I IFN response has been reported to play an important role in the development and severity of human and murine lupus(3, 7, 23, 24). In the pristane model of lupus, type I IFN pathways are required for disease development, as mice lacking the type I IFN receptor, TLR7 or IRF5 do not develop a clinical phenotype(6, 7, 20, 25). Type I IFN responses were examined in the spleens and bone marrow of WT and caspase-1 −/− mice 2

weeks and six months after exposure to pristane. As shown in figure 2A, at two weeks after pristane exposure there were no significant differences in type I IFN responses between WT and caspase-1 −/− mice. In contrast, WT, but not caspase-1 −/−, splenocytes and bone marrow cells isolated 6 months after treatment displayed significant upregulation of type I IFN-regulated genes when compared to PBS exposed littermates. This repression in IFN signatures was not secondary to alterations in signaling through the TLR7 receptor, as exposure to the TLR7 ligand R848 resulted in similar upregulation of type I IFN-regulated genes in WT and caspase-1 −/− mice (Figure 2B). Further, as an important role for inflammatory monocytes in initiation of type I IFN responses in the pristane model has been demonstrated(26), we examined whether differences in IFN signatures of these cells occurred in pristane-exposed WT and caspase-1 −/− mice. No significant differences in the IFN signature of peritoneal inflammatory cells were noted between wild-type and caspase-1 −/− mice two weeks post pristane exposure (data not shown). These results indicate that lack of caspase-1 triggers repression of type I IFN signatures in pristane-treated mice.

The aberrant clearance of apoptotic debris in SLE may lead to autoantigen exposure and promotion of the type I IFN response and autoimmune pathways(27). Pristane exposure induces various forms of cell death, including NETosis in neutrophils and apoptosis in various inflammatory cells in the peritoneal cavity(18). Therefore, we examined whether absence of caspase-1 modified cell death responses two weeks following pristane injection. We were unable to detect spontaneous NET formation in neutrophils isolated directly from the peritoneum after pristane exposure. In contrast, robust NET formation was observed following PMA stimulation of bone-marrow derived neutrophils from WT and caspase-1 −/− mice, suggesting that caspase-1 does not influence the NET response (Figure 2D).

In order to evaluate the role of caspase-1 in pristane-induced apoptosis and pyroptosis (inflammatory cell death), we utilized Annexin V staining of peritoneal inflammatory cells isolated two weeks after pristane exposure. We detected a significant decrease in Annexin V staining, which recognizes both apoptotic and pyroptotic cells(28), in peritoneal cells isolated from caspase-1 −/− mice when compared to WT (Figure 2E), suggesting that cell death following pristane exposure is abrogated in caspase-1 −/− mice. As aberrant cell death is considered an important phenomenon in modified autoantigen externalization, the formation of immune complexes and the development of enhanced type I IFN responses(27), our observations suggest that caspase-1 may play an important role in regulating type I IFN synthesis by modulating cell death pathway.

Absence of caspase-1 decreases markers of CV risk

The inflammasome has been implicated in inflammatory responses in atherosclerotic plaques(29), and lack of caspase-1 modulates severity of atheroma in murine models(30). We previously demonstrated that in vitro inhibition of caspase-1 improves the differentiation of EPCs to mature endothelial cells (ECs) in lupus patients, a phenomenon that may be important in preventing vascular damage in this disease(4, 31, 32). Thus, we examined whether lack of caspase-1 modified CV parameters in the pristane-induced lupus model. Both mice in the Balb/c and C57BL/6 backgrounds were studied, as lupus models of various backgrounds display endothelial dysfunction to varying degrees(33). Neither exposure to

pristane nor absence of caspase-1 altered the number of bone marrow EPCs, as assessed by flow cytometry (Figure 3A). However, absence of caspase-1 significantly abrogated the inhibitory effects on EPC differentiation induced by pristane (Figures 3B–C). These observations confirm previous in vitro data in humans and indicate that caspase-1 is operational in vivo with regards to lupus-mediated EPC dysfunction. Previously, we also showed that other murine models of lupus display impaired endothelial-dependent vasorelaxation, a phenomenon associated with progression to atherosclerosis in human systems(33). In pristane-treated C57BL/6 mice, but not in pristane-treated Balb/c mice, a similar decrease in endothelium-dependent vasorelaxation was observed following exposure to pristane. However, both Balb/c and C57BL/6 caspase-1 −/− mice displayed significant increases in endothelium-dependent vasorelaxation when compared to WT, following PBS or pristane exposure (Figure 3D). These results indicate that caspase-1 modulates the vasodilatory capacity of the endothelium, independent of lupus-phenotype or mouse strain.

Caspase-1 is required for the development of immune-complex glomerulonephritis in pristane-induced lupus

As expected, pristane exposure resulted in prominent immune complex deposition in the glomeruli of WT Balb/c mice. In contrast, caspase-1 −/− mice had significant decreases in glomerular immune complex deposition (Figure 4A–B). Furthermore, lack of caspase-1 protected Balb/c mice exposed to pristane from glomerular inflammation (Figure 4C–D). Decreases in immune complex deposition and renal inflammation in caspase-1 −/− mice significantly correlated with decreases in titers of anti-dsDNA, anti-RNP and total IgG titers (not shown). While WT Balb/c mice trended toward increased albuminuria following pristane exposure, caspase-1 −/− mice did not have similar increases after pristane exposure (Figure 4E). Similar patterns were found when examining total protein/creatinine ratios (not shown). Further, WT, but not caspase-1 −/−, mice exposed to pristane had a trend for increased serum IL-18 levels, and the serum concentration of IL-18 significantly correlated with the severity of nephritis in WT pristane-exposed mice (Figure 4F and G). These results indicate that glomerular immune complex deposition and renal inflammation are hampered in the absence of caspase-1 and that activation of IL-18 by caspase-1 may be an important step in nephritis induction in this model.

Discussion

The development of lupus is considered to be the result of an aberrant interplay between innate and adaptive immune responses. Recently, the inflammasome machinery has been proposed to be dysregulated in lupus systems secondary to type I IFN, aberrant cell death and autoantibody-mediated effects(4, 10–12, 34). Results presented in this manuscript identify novel roles for caspase-1, the central enzyme of the inflammasome, in the pristane-induced lupus model. Indeed, absence of caspase-1 abrogated known hallmarks of murine and human SLE, including autoantibody development, type I IFN signatures and renal inflammation.

There are likely several mechanisms by which caspase-1 modulates lupus development. Serum levels of IL-18 are elevated in SLE patients and have been correlated with disease

severity and lupus nephritis(17, 35, 36), and in the MRL-*Fas*^{lpr} lupus model a role for IL-18 in nephritis and skin disease has been proposed(37). IL-18 regulates IFNγ production (38), and this may further modulate SLE development as IFNγ is required for disease pathology(39). Upregulation of IL-1β and IL-18 transcripts in response to pristane was not observed in caspase-1 −/− mice, suggesting that pristane may require caspase-1-dependent pathways to induce these cytokines. Additionally, the severity of nephritis significantly correlated with serum levels of IL-18 in these mice suggesting that caspase-1 activation of IL-18 may play a pathogenic role in nephritis induction.

Despite the profound impact on lupus development, lack of caspase-1 did not impact peritoneal inflammatory responses to pristane. Indeed, an enhanced neutrophil recruitment was observed in the peritoneal cavity of pristine-treated caspase-1 −/− mice. Previously, the recruitment of neutrophils following pristane exposure has been shown to be dependent on IL-1α-mediated upregulation of CXCL5/RANTES(40). This cytokine is secreted in a caspase-1-dependent manner and expressed on the cell surface in a caspase-1 independent manner. Cell surface IL-1α is increased following inhibition of caspase-1(41); thus, the paradoxical increase in neutrophils seen in caspase-1 −/− mice may be secondary to increased expression of surface IL-1α. Additionally, increased surface IL-1α in the absence of caspase-1 may explain the enhanced basal CXCL5/RANTES expression seen in caspase-1 −/− mice.

The induction of accelerated cell death and aberrant uptake of apoptotic debris has been postulated as a mechanism for lupus induction(27). Thus, lack of caspase-1 may be protective against inflammatory responses initiated by apoptotic debris. Furthermore, in addition to its role as activator of IL-1β and IL-18, caspase-1 is also required for induction of inflammatory cell death, also known as pyroptosis. While traditionally activated by intracellular bacterial infection, activation of caspase-1-dependent cell death may also be a relevant physiologic cell death pathway (reviewed in(42)). Importantly, the phagocytosis of pyroptotic debris may occur through similar “eat me” signals employed by apoptotic cells(28). We hypothesize that aberrant clearance of pyroptotic debris may also contribute to SLE pathogenesis. Our data show decreased Annexin V staining of inflammatory cells following pristane exposure in caspase-1 −/− mice, which detects both apoptotic and pyroptotic debris(28). As such, downregulation of inflammatory cell death following pristane exposure may decrease autoantigen externalization, limit aberrant autoantibody formation and decrease type I IFN synthesis. Future studies should further test this hypothesis.

Caspase-1 −/− mice exposed to pristane lack significant autoantibody development. Because autoreactive B cells are activated by ribonucleoprotein autoantigens(43), the abrogation of cell death pathways in caspase-1 −/− mice likely decreases B cell activation. Further, the profound lack of chronic type I IFN upregulation in caspase-1 −/− mice may have negative effects on B cells as type I IFN production is an important mediator of B cell activation and class switching(44). Decreased IL-6 production in caspase-1 −/− mice may also contribute to lower autoantibody titers, given that this cytokine has been reported to synergize with type I IFN responses to induce B cell maturation into highly functional IgG secreting plasma cells(45), as well as to promote many other pro-inflammatory responses.

The role of caspase-1 may not only relate to autoantibody development in response to pristane but also to downstream responses to immune complexes. Recently, activation of the inflammasome via U1-small nuclear RNP/anti-RNP complexes through TLR7 stimulation was described in human monocytes(11), and similar responses occur in response to dsDNA Ab complexes(12). Further, caspase-1 activation is enhanced in SLE macrophages in response to neutrophil NETs(10). The associated cytokine generation further enhances inflammatory responses and NET formation, which can result in circulating immune complexes capable of stimulating pDC activation and type I IFN production(46). Thus, caspase-1 likely plays important roles in both autoantibody generation and inflammatory responses downstream of immune complexes.

With regards to the role of caspase-1 in SLE-associated CVD, lack of caspase-1 improved EPC differentiation in the pristane-induced model. This supports our previous observations that inhibition of caspase-1 provides a vasculoprotective effect in human SLE(4). Others have demonstrated similar effects on atherosclerosis development in apolipoprotein-E-null mice(30). Endothelium-dependent vasorelaxation was increased in the absence of caspase-1, independent of mouse strain or lupus phenotype. The mechanisms behind this enhanced relaxation in the caspase-1 −/− mice may be secondary to a combination of decreased endothelial damage and enhanced vascular repair. The inflammasome plays a role in response to cholesterol crystals and generation of inflammatory responses in plaque(29). Without active caspase-1, the negative effects of vascular inflammation on the endothelium are likely dampened. Further, type I IFNs and IL-18 have negative effects on vascular repair(2, 4, 47). As caspase-1 −/− mice have repressed type I IFN responses and do not activate IL-18, this may lead to improved EPC differentiation and endothelial function. Additional studies are nevertheless require to further define how caspase-1 inhibition improves vascular function in murine and human systems(47–49).

This study has some limitations. The experimental design addresses the role of caspase-1 in pristane-induced lupus, but it does not provide information on specific activation of the inflammasome in this model. Additionally, recent observations on the caspase-1 −/− mouse revealed that it contains a non-functional caspase-11 gene(50). While not required for classical inflammasome activation, caspase-11 may be important for pathogen-induced inflammasome assembly and in mediating pyroptosis in response to infection(50). Further experiments to address the role of caspase-11 specifically in the pristane lupus model should be explored.

In summary, we have demonstrated a role for caspase-1 in the development of murine lupus characterized by significant downmodulation of autoantibody synthesis, type I IFN responses, glomerulonephritis and vascular dysfunction. These results indicate the need to further explore the inflammasome as a putative therapeutic target in this disease.

Acknowledgments

Financial Support: This work was supported by the Alliance for Lupus Research and by the National Institutes of Health (NIH) through Public Health Service (PHS) grant HL088419 (both to MJK). Support to JMK was provided through the American College of Rheumatology Rheumatology Research Foundation. JBH received support through the NIH via PHS grant K08DK088944.

References

1. Ward MM. Premature morbidity from cardiovascular and cerebrovascular diseases in women with systemic lupus erythematosus. Arthritis Rheum. 1999; 42(2):338–346. [PubMed: 10025929]
2. Denny MF, Thacker S, Mehta H, Somers EC, Dodick T, Barrat FJ, et al. Interferon-alpha promotes abnormal vasculogenesis in lupus: a potential pathway for premature atherosclerosis. Blood. 2007; 110(8):2907–2915. [PubMed: 17638846]
3. Kirou K, Lee C, George S, Louca K, Peterson MGE, Crow M. Activation of the interferon-alpha pathway identifies a subgroup of systemic lupus erythematosus patients with distinct serologic features and active disease. Arthritis and rheumatism. 2005; 52(5):1491–1503. [PubMed: 15880830]
4. Kahlenberg JM, Thacker SG, Berthier CC, Cohen CD, Kretzler M, Kaplan MJ. Inflammasome activation of IL-18 results in endothelial progenitor cell dysfunction in systemic lupus erythematosus. J Immunol. 2011; 187(11):6143–6156. [PubMed: 22058412]
5. Reeves WH, Lee PY, Weinstein JS, Satoh M, Lu L. Induction of autoimmunity by pristane and other naturally occurring hydrocarbons. Trends Immunol. 2009; 30(9):455–464. [PubMed: 19699150]
6. Lee PY, Kumagai Y, Li Y, Takeuchi O, Yoshida H, Weinstein J, et al. TLR7-dependent and FcγR-independent production of type I interferon in experimental mouse lupus. The Journal of experimental medicine. 2008; 205(13):2995–3006. [PubMed: 19047436]
7. Thibault D, Graham K, Lee L, Balboni I, Hertzog P, Utz P. Type I interferon receptor controls B-cell expression of nucleic acid-sensing Toll-like receptors and autoantibody production in a murine model of lupus. Arthritis research & therapy. 2009; 11(4):R112-R. [PubMed: 19624844]
8. Lee PY, Li Y, Kumagai Y, Xu Y, Weinstein JS, Kellner ES, et al. Type I Interferon Modulates Monocyte Recruitment and Maturation in Chronic Inflammation. The American Journal of Pathology. 2009; 175(5):2023–2033. [PubMed: 19808647]
9. Lamkanfi M, Dixit VM. Inflammasomes and Their Roles in Health and Disease. Annual Review of Cell and Developmental Biology. 2012; 28(1):137–161.
10. Kahlenberg JM, Carmona-Rivera C, Smith CK, Kaplan MJ. Neutrophil Extracellular Trap–Associated Protein Activation of the NLRP3 Inflammasome Is Enhanced in Lupus Macrophages. The journal of immunology. 2013; 190(3):1217–1226. [PubMed: 23267025]
11. Shin MS, Kang Y, Lee N, Kim SH, Kang KS, Lazova R, et al. U1-Small Nuclear Ribonucleoprotein Activates the NLRP3 Inflammasome in Human Monocytes. The journal of immunology. 2012; 188(10):4769–4775. [PubMed: 22490866]
12. Shin MS, Kang Y, Lee N, Wahl ER, Kim SH, Kang KS, et al. Self Double-Stranded (ds)DNA Induces IL-1β Production from Human Monocytes by Activating NLRP3 Inflammasome in the Presence of Anti–dsDNA Antibodies. The journal of immunology. 2013
13. Zhao W, Thacker SG, Hodgin JB, Zhang H, Wang JH, Park JL, et al. The peroxisome proliferator-activated receptor gamma agonist pioglitazone improves cardiometabolic risk and renal inflammation in murine lupus. J Immunol. 2009; 183(4):2729–2740. [PubMed: 19620300]
14. Boxio R, Bossenmeyer-Pourie C, Steinckwich N, Dournon C, Nusse O. Mouse bone marrow contains large numbers of functionally competent neutrophils. J Leukoc Biol. 2004; 75(4):604–611. [PubMed: 14694182]
15. Villanueva E, Yalavarthi S, Berthier CC, Hodgin JB, Khandpur R, Lin AM, et al. Netting neutrophils induce endothelial damage, infiltrate tissues, and expose immunostimulatory molecules in systemic lupus erythematosus. J Immunol. 2011; 187(1):538–552. [PubMed: 21613614]
16. Liu X, Bao C, Hu D. Elevated interleukin-18 and skewed Th1:Th2 immune response in lupus nephritis. Rheumatology international. 2010:1–7. [PubMed: 21120502]
17. Tucci M, Quatraro C, Lombardi L, Pellegrino C, Dammacco F, Silvestris F. Glomerular accumulation of plasmacytoid dendritic cells in active lupus nephritis: role of interleukin-18. Arthritis and rheumatism. 2008; 58(1):251–262. [PubMed: 18163476]

18. Herman S, Kny A, Schorn C, Pfatschbacher J, Niederreiter B, Herrmann M, et al. Cell death and cytokine production induced by autoimmunogenic hydrocarbon oils. Autoimmunity. 2012; 45(8): 602–611. [PubMed: 22917079]
19. Yang L, Feng D, Bi X, Stone RC, Barnes BJ. Monocytes from irf5−/− mice have an intrinsic defect in their response to pristane-induced lupus. J Immunol. 2012; 189(7):3741–3750. [PubMed: 22933628]
20. Xu Y, Lee PY, Li Y, Liu C, Zhuang H, Han S, et al. Pleiotropic IFN-dependent and -independent effects of IRF5 on the pathogenesis of experimental lupus. J Immunol. 2012; 188(8):4113–4121. [PubMed: 22422888]
21. Weinstein JS, Delano MJ, Xu Y, Kelly-Scumpia KM, Nacionales DC, Li Y, et al. Maintenance of anti-Sm/RNP autoantibody production by plasma cells residing in ectopic lymphoid tissue and bone marrow memory B cells. J Immunol. 2013; 190(8):3916–3927. [PubMed: 23509349]
22. Feng D, Yang L, Bi X, Stone RC, Patel P, Barnes BJ. Irf5-deficient mice are protected from pristine-induced lupus via increased Th2 cytokines and altered IgG class switching. Eur J Immunol. 2012; 42(6):1477–1487. [PubMed: 22678902]
23. Weckerle CE, Franek BS, Kelly JA, Kumabe M, Mikolaitis RA, Green SL, et al. Network analysis of associations between serum interferon-alpha activity, autoantibodies, and clinical features in systemic lupus erythematosus. Arthritis Rheum. 2011; 63(4):1044–1053. [PubMed: 21162028]
24. Agrawal H, Jacob N, Carreras E, Bajana S, Putterman C, Turner S, et al. Deficiency of type I IFN receptor in lupus-prone New Zealand mixed 2328 mice decreases dendritic cell numbers and activation and protects from disease. The journal of immunology. 2009; 183(9):6021–6029. [PubMed: 19812195]
25. Savarese E, Steinberg C, Pawar R, Reindl W, Akira S, Anders H-J, et al. Requirement of Toll-like receptor 7 for pristane-induced production of autoantibodies and development of murine lupus nephritis. Arthritis and rheumatism. 2008; 58(4):1107–1115. [PubMed: 18383384]
26. Lee PY, Weinstein JS, Nacionales DC, Scumpia PO, Li Y, Butfiloski E, et al. A novel type I IFN-producing cell subset in murine lupus. J Immunol. 2008; 180(7):5101–5108. [PubMed: 18354236]
27. White S, Rosen A. Apoptosis in systemic lupus erythematosus. Curr Opin Rheumatol. 2003; 15(5): 557–562. [PubMed: 12960480]
28. Wang Q, Imamura R, Motani K, Kushiyama H, Nagata S, Suda T. Pyroptotic cells externalize eat-me and release find-me signals and are efficiently engulfed by macrophages. International Immunology. 2013
29. Duewell P, Kono H, Rayner KJ, Sirois CM, Vladimer G, Bauernfeind FG, et al. NLRP3 inflammasomes are required for atherogenesis and activated by cholesterol crystals. Nature. 2010; 464(7293):1357–1361. [PubMed: 20428172]
30. Gage J, Hasu M, Thabet M, Whitman SC. Caspase-1 Deficiency Decreases Atherosclerosis in Apolipoprotein E-Null Mice. Canadian Journal of Cardiology. 2012; 28(2):222–229. [PubMed: 22265992]
31. Briasoulis A, Tousoulis D, Antoniades C, Papageorgiou N, Stefanadis C. The Role of Endothelial Progenitor Cells in Vascular Repair after Arterial Injury and Atherosclerotic Plaque Development. Cardiovascular Therapeutics. 2011; 29(2):125–139. [PubMed: 20406237]
32. Vasa M, Fichtlscherer S, Aicher A, Adler K, Urbich C, Martin H, et al. Number and migratory activity of circulating endothelial progenitor cells inversely correlate with risk factors for coronary artery disease. Circulation research. 2001; 89(1):E1–E7. [PubMed: 11440984]
33. Thacker SG, Duquaine D, Park J, Kaplan MJ. Lupus-prone New Zealand Black/New Zealand White F1 mice display endothelial dysfunction and abnormal phenotype and function of endothelial progenitor cells. Lupus. 2010; 19(3):288–299. [PubMed: 20068018]
34. Zhang W, Cai Y, Xu W, Yin Z, Gao X, Xiong S. AIM2 Facilitates the Apoptotic DNA-induced Systemic Lupus Erythematosus via Arbitrating Macrophage Functional Maturation. Journal of clinical immunology. 2013:1–13. [PubMed: 22847546]
35. Hu D, Liu X, Chen S, Bao C. Expressions of IL-18 and its binding protein in peripheral blood leukocytes and kidney tissues of lupus nephritis patients. Clin Rheumatol. 2010; 29(7):717–721. [PubMed: 20140691]

36. Calvani N, Richards HB, Tucci M, Pannarale G, Silvestris F. Up-regulation of IL-18 and predominance of a Th1 immune response is a hallmark of lupus nephritis. Clinical and experimental immunology. 2004; 138(1):171–178. [PubMed: 15373921]
37. Kinoshita K, Yamagata T, Nozaki Y, Sugiyama M, Ikoma S, Funauchi M, et al. Blockade of IL-18 Receptor Signaling Delays the Onset of Autoimmune Disease in MRL-Faslpr Mice. The journal of immunology. 2004; 173(8):5312–5318. [PubMed: 15470078]
38. Lee J-K, Kim S-H, Lewis EC, Azam T, Reznikov LL, Dinarello CA. Differences in signaling pathways by IL-1β and IL-18. Proceedings of the National Academy of Sciences of the United States of America. 2004; 101(23):8815–8820. [PubMed: 15161979]
39. Richards HB, Satoh M, Jennette JC, Croker BP, Yoshida H, Reeves WH. Interferon-[ggr] is required for lupus nephritis in mice treated with the hydrocarbon oil pristane. Kidney Int. 2001; 60(6):2173–2180. [PubMed: 11737591]
40. Lee PY, Kumagai Y, Xu Y, Li Y, Barker T, Liu C, et al. IL-1α Modulates Neutrophil Recruitment in Chronic Inflammation Induced by Hydrocarbon Oil. The journal of immunology. 2011; 186(3): 1747–1754. [PubMed: 21191074]
41. Fettelschoss A, Kistowska M, LeibundGut-Landmann S, Beer H-D, Johansen P, Senti G, et al. Inflammasome activation and IL-1β target IL-1α for secretion as opposed to surface expression. Proceedings of the National Academy of Sciences. 2011; 108(44):18055–18060.
42. Denes A, Lopez-Castejon G, Brough D. Caspase-1: is IL-1 just the tip of the ICEberg[quest]. Cell Death Dis. 2012; 3:e338. [PubMed: 22764097]
43. Green NM, Moody K-S, Debatis M, Marshak-Rothstein A. Activation of Autoreactive B Cells by Endogenous TLR7 and TLR3 RNA Ligands. Journal of Biological Chemistry. 2012; 287(47): 39789–39799. [PubMed: 23019335]
44. Swanson CL, Wilson TJ, Strauch P, Colonna M, Pelanda R, Torres RM. Type I IFN enhances follicular B cell contribution to the T cell–independent antibody response. The Journal of experimental medicine. 2010; 207(7):1485–1500. [PubMed: 20566717]
45. Jego G, Palucka AK, Blanck J-P, Chalouni C, Pascual V, Banchereau J. Plasmacytoid Dendritic Cells Induce Plasma Cell Differentiation through Type I Interferon and Interleukin 6. Immunity. 2003; 19(2):225–234. [PubMed: 12932356]
46. Lande R, Ganguly D, Facchinetti V, Frasca L, Conrad C, Gregorio J, et al. Neutrophils Activate Plasmacytoid Dendritic Cells by Releasing Self-DNA-Peptide Complexes in Systemic Lupus Erythematosus. Sci Transl Med. 2011; 3(73):73ra19.
47. Thacker SG, Zhao W, Smith CK, Luo W, Wang H, Vivekanandan-Giri A, et al. Type I interferons modulate vascular function, repair, thrombosis and plaque progression in murine models of lupus and atherosclerosis. Arthritis & Rheumatism. 2012 n/a-n/a.
48. Kahlenberg JM, Kaplan MJ. The interplay of inflammation and cardiovascular disease in systemic lupus erythematosus. Arthritis Res Ther. 2011; 13(1):203. [PubMed: 21371346]
49. Niessner A, Weyand CM. Dendritic cells in atherosclerotic disease. Clinical Immunology. 2010; 134(1):25–32. [PubMed: 19520615]
50. Kayagaki N, Warming S, Lamkanfi M, Walle LV, Louie S, Dong J, et al. Non-canonical inflammasome activation targets caspase-11. Nature. 2011; 479(7371):117–121. [PubMed: 22002608]

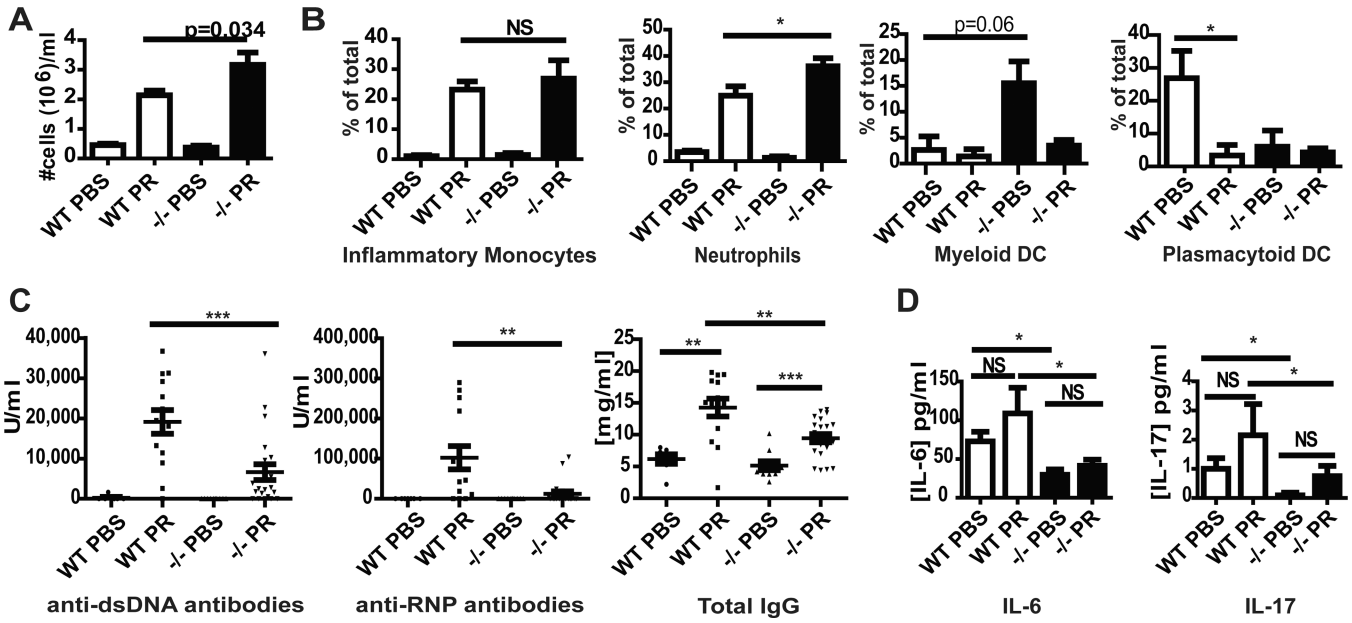

Figure 1.

Balb/c Caspase-1 −/− mice have intact peritoneal inflammatory responses to pristane injection but display decreased autoantibody, inflammatory cytokine and chemokine synthesis. A and B. Wild-type (WT) (n=4 PBS, n=10 pristane) and Caspase-1 −/− (n=5 PBS, n=11 pristane) peritoneal fluid was harvested 2 weeks post pristane or PBS injection. A. Total cell numbers were counted and are plotted as mean+SEM cell number per ml of peritoneal fluid removed. B. Cell populations were quantified by flow cytometry and are expressed as percentage of the total cell population when $1x10^6$ total cells are examined. C. Results represent quantification of antibody titers by ELISA of sera from wild-type (WT) Balb/c or Balb/c caspase-1 −/− mice six months post exposure to PBS or pristane. Each dot represents a single mouse and mean +/− SEM is plotted. PBS WT n=6, PBS −/− n=11, Pristane WT n=13, Pristane −/− n=24. D. Plasma cytokine and chemokine concentrations from mice described in (C) were quantified on undiluted samples using Milliplex. Bars represent the mean +SEM. PBS WT n=6, PBS −/− n=11, Pristane WT n=13, Pristane −/− n=24. *=p<0.05, **=p<0.01, ***=p<0.001. PR=pristane

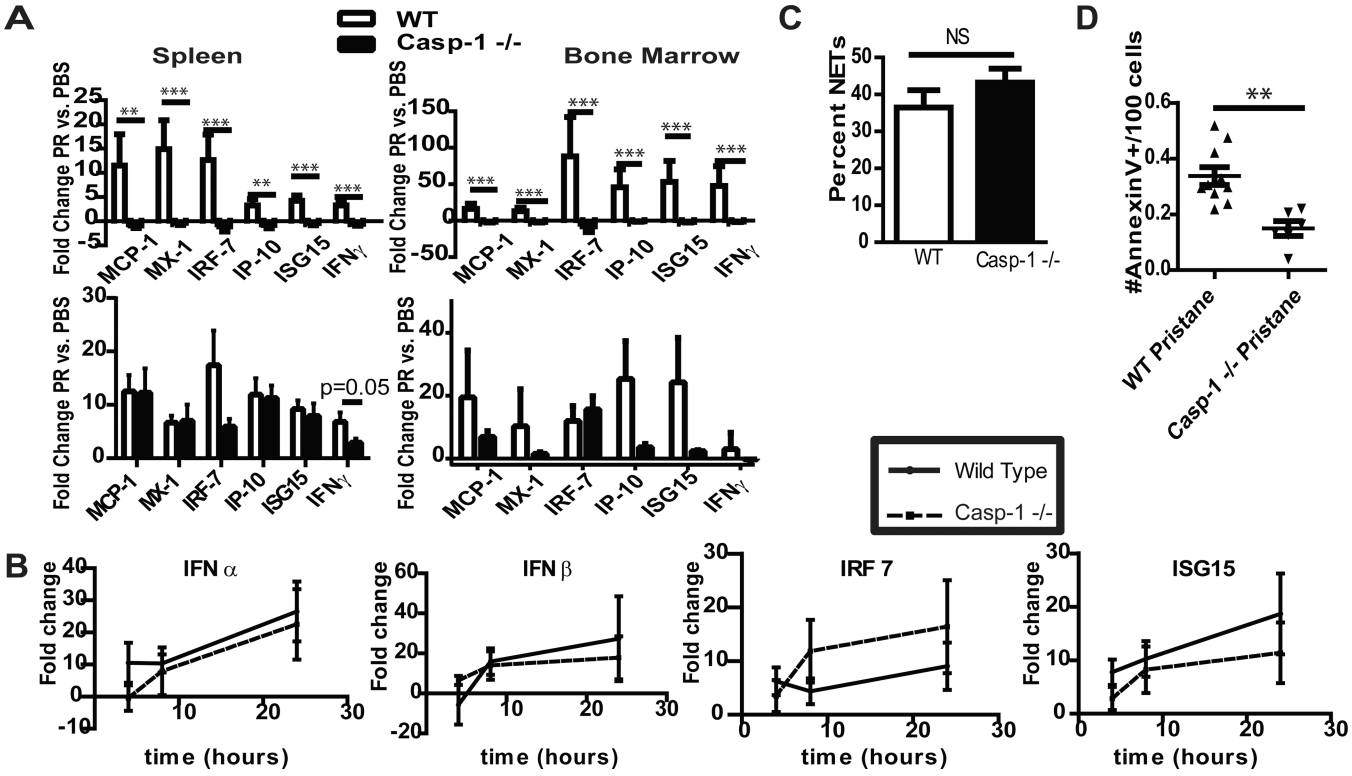

Figure 2.

Type I IFN signature induced after pristane exposure is abrogated in caspase-1 −/− mice. A. Bars represent mean fold-change +SEM mRNA of type I IFN regulated genes in splenocytes and bone marrow mononuclear cells isolated from Balb/c mice 6 months (top) or 2 weeks (bottom) after treatment. Following normalization to β-actin, comparisons of δ-CT were made for pristane versus PBS-treated mice. PBS WT n=7, PBS −/− n=11, Pristane WT n=14, Pristane −/− n=24. B. WT Balb/c or caspase-1 −/− (n=5 each) splenocytes from 10 week-old mice were stimulated with R848 for varying time points. Quantification of mRNA of type I IFN-regulated genes was performed as in 2A. C. Bone marrow neutrophils were isolated from WT or caspase-1 −/− mice (n=4 each) and stimulated overnight with 40nM PMA. NETs were detected by extracellular colocalization of anti-elastase and Hoechst. Graph represents mean +SEM of percent of NETs calculated as number of NETting cells/ total number of cells. D. Two weeks following pristane injection, peritoneal inflammatory cells were isolated, stained with Annexin-V and analyzed via flow cytometry. Graph demonstrates # apoptotic/pyroptotic cells/100 cells in the live cell gate for each mouse (WT n=10, caspase-1 −/−, n=6). **=p<0.01, ***=p<0.001.

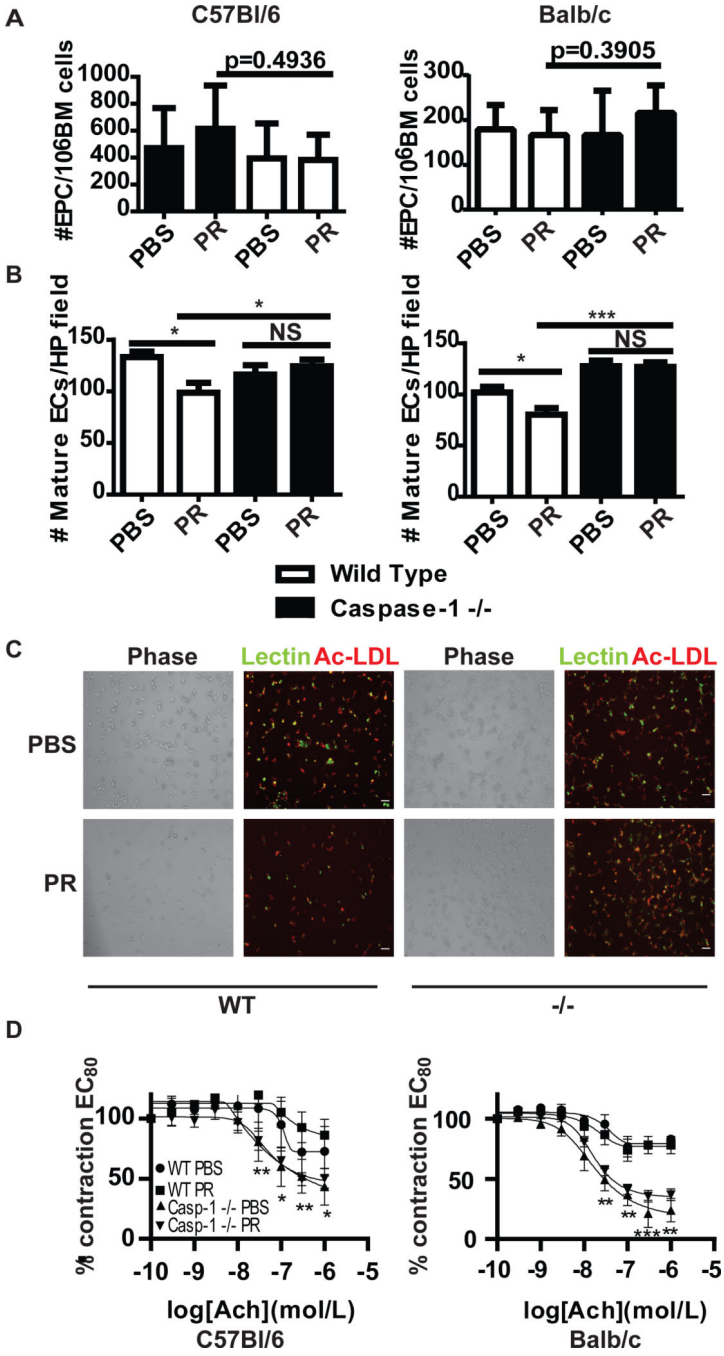

Figure 3.

EPC differentiation and endothelial-dependent vasorelaxation increase in the absence of caspase-1. A. Bone marrow from (left) C57BL/6 WT (n=5 PBS, n=8 pristane) or C57BL/6 caspase-1 −/− mice (n=10 PBS, n=14 pristane) or (right) Balb/c WT (n=7 PBS, n=14 pristane) or Balb/c caspase-1 −/− (n=11 PBS, n=24 pristane) mice was isolated and EPCs were quantified by flow cytometry. Results represent the mean+SEM of EPCs/ml of blood for each group. B. Bars represent number of mature endothelial cells (ECs)/high power field quantified by fluorescent microscopy 7 days after plating bone marrow cells under

proangiogenic conditions. Left figure represents C57BL/6 WT (n=5 PBS, n=8 pristane) compared to C57BL/6 caspase-1 −/− mice (n=10 PBS, n=14 pristane). Right figure represents Balb/c WT (n=7 PBS, n=14 pristane) versus Balb/c caspase-1 −/− (n=11 PBS, n=24 pristane) mice. C. Representative photomicrograph of EC cultures as in B. D. Following establishment of maximal contraction, endothelium-dependent vasorelaxation of aortic rings was quantified following exposure to graded concentrations of Acetylcholine (Ach) to 80% contracted aortic rings. p values represent comparisons between WT and caspase-1 −/− mice. n=3 PBS WT, 6 PBS pristane, 11 PBS casp-1 −/− and 23 pristane casp-1 −/−. *=$p<0.05$, **=$p<0.01$, ***=$p<0.001$.

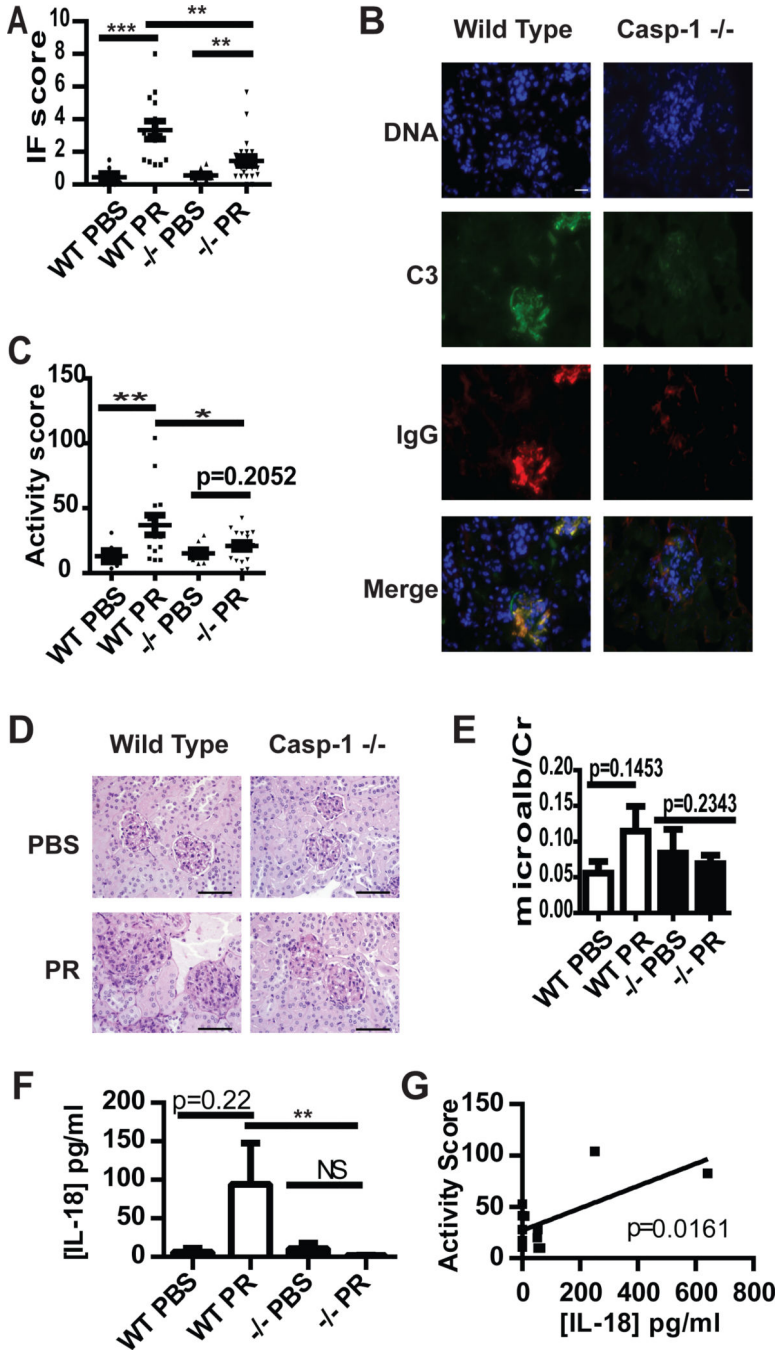

Figure 4.

Caspase-1 modulates immune complex deposition and glomerular activity scores in lupus-prone mice. A and B. Deposition of C3 (green) and IgG (red) was quantified in kidneys obtained from WT Balb/c or caspase-1 −/− mice following PBS or pristane exposure. Composite scores were averaged (A) and representative photomicrographs are shown in B. Each kidney is represented on the graph and the mean+/−SEM is displayed. PBS WT n=7, PBS −/− n=11, Pristane WT n=14, Pristane −/− n=23. Scale bar=20μm. C and D. Glomerular inflammation activity scores were determined on PAS-stained formalin-fixed

kidney sections from WT or caspase-1−/− mice exposed to PBS or pristane and displayed as in A. Representative photomicrographs (D) demonstrate enlarged, hypercellular glomeruli in pristane WT mice, but not in caspase-1 −/− mice, due to mesangial and endocapillary inflammation. WT PBS n=6, PBS −/− n=8, Pristane WT n=14, Pristane −/− n=19. Scale bars=100μm. E. Microalbumin:creatinine ratios were determined on urine collected at the time of euthanasia. n=as in A. F. [IL-18] was determined by ELISA on serum collected 5 months post PBS or pristane treatment. n= as in A. G. Linear regression of [IL-18] vs. renal activity score in pristane treated WT mice (n=12). *=$p<0.05$, **=$p<0.01$, ***=$p<0.001$. PR=pristane.

Table 1

Mean fold increase ± SEM of splenic inflammatory transcripts 6 months post pristane injection in WT and Casp-1 −/− mice

P value calculated by comparison of δCT between PBS (n=7 WT and 11 casp-1 −/−) and Pristane (n=13 WT and n=23 casp-1 −/−) treated samples. NLRP3=NOD-like receptor family pyrin domain-containing 3, CASP1=caspase-1, IL- 1β=interleukin-1 beta, IL-18=interleukin 18. PBS WT n=6, PBS −/− n=11, Pristane WT n=13, Pristane −/− n=24.

	Wild Type		Caspase-1 −/−	
Gene	**Fold Change**	**p value**	**Fold Change**	**p value**
NLRP3	19.70±8.352	0.0020	−.4845±0.6457	0.6753
CASP1	4.964±2.034	0.0456	----------	---------
IL-1β	106.4±71.77	0.1418	−43.40±37.77	0.4351
IL-18	404.8±286.4	0.0813	−14.53±6.682	0.3358

Table 2

Levels ± SEM of plasma chemokines and cytokines of Balb/c wild-type or Balb/c caspase-1 KO mice six months following exposure to PBS or pristine

MCP-1=monocyte chemoattractant protein 1/CCL2; MIP1α=macrophage inflammatory protein 1α/CCL3; IP-10=interferon gamma-induced protein-10/CXCL10; CCL=chemokine ligand; GMCSF=granulocyte macrophage colony stimulating factor; IFN=interferon; IL=interleukin; TNF=tumor necrosis factor. PBS WT n=6, PBS −/− n=11, Pristane WT n=13, Pristane −/− n=24.

Cytokine	Wild Type PBS (pg/ml)	Wild Type Pristane (pg/ml)	WT PBS vs Pristane p value	Casp-1 −/− PBS (pg/ml)	Casp-1 −/− Pristane (pg/ml)	Casp-1 −/− PBS vs Pristane p value	WT pristane vs KO pristane p value
MCP-1	36±10.37	174.8±25.86	**0.0024**	78.36±78.36	124.4±16.1	0.0251	0.0856
MIP1α	9.5±5.051	45±10.57	**0.0105**	1.83±1.273	14.23±2.425	**0.0004**	**0.0009**
IP-10	205±49.12	332.8±29.11	**0.0393**	163.7±25.16	335.8±42.63	**0.0007**	NS
CCL5/rantes	18.17±5.474	18.92±3.68	NS	51.09±27.07	63.67±25.35	NS	**0.0371**
GMCSF	75.17±18.4	85.00±25.38	NS	53.40±16.45	80.08±25.13	NS	NS
IFN-γ	0.6667±0.494	0.6154±0.368	NS	0.8000±0.467	1.292±0.682	NS	NS
IL-1β	9.000±4.025	4.154±2.189	NS	8.900±3.761	3.167±1.788	NS	NS
IL-2	26.83±7.639	19.46±8.883	NS	8.545±4.137	7.875±2.23	NS	NS
IL-4	0	.07692±0.077	NS	0	0	NS	NS
IL-5	4.5±2.986	11.23±3.327	NS	9.273±4.083	6.833±2.103	NS	NS
IL-10	0	0	NS	11.18±11.18	11.79±9.548	NS	NS
IL-12p40	27.33±9.535	57.62±42.07	NS	42.45±11.89	80.21±53.55	NS	NS
IL-12p70	5.333±2.894	261.6±229.8	NS	2.545±1.065	11.13±8.632	NS	NS
TNF-α	2.5±1.586	4.615±1.357	NS	4.182±1.536	3.25±0.7	NS	NS